J. Sens. Sens. Syst., 5, 165–170, 2016
www.j-sens-sens-syst.net/5/165/2016/
doi:10.5194/jsss-5-165-2016

JSSS Journal of Sensors and Sensor Systems Open Access

Characterisation of the polarisation state of embedded piezoelectric transducers by thermal waves and thermal pulses

Agnes Eydam, Gunnar Suchaneck, and Gerald Gerlach

Solid State Electronics Laboratory, Technische Universität Dresden, Dresden, Germany

Correspondence to: Agnes Eydam (agnes.eydam@tu-dresden.de)

Received: 8 October 2015 – Revised: 22 January 2016 – Accepted: 4 April 2016 – Published: 10 May 2016

Abstract. In this work, we apply the thermal wave method and the thermal pulse method for non-destructive characterisation of the polarisation state of embedded piezoelectric transducers. Heating the sample with a square-wave modulated laser beam or a single laser pulse leads to a pyroelectric current recorded in the frequency or time domain, respectively. It carries information about the polarisation state. Analytical and numerical finite element models describe the pyroelectric response of the piezoceramic. Modelling and experimental results are compared for a simple lead–zirconate–titanate (PZT) plate, a low-temperature co-fired ceramics (LTCC)/PZT sensor and actuator, and a macro-fibre composite (MFC) actuator.

1 Introduction

Piezoelectric smart structures are created by embedding piezoelectric transducers into structural components to make them controllable or responsive to their environment. These structures find applications, for instance, for health-monitoring of safety components, for reducing noise emission in automobile engineering, or for damping vibrations. Their mass-production requires control of the polarisation state due to mechanical and thermal loads appearing during device fabrication.

Non-destructive methods for obtaining polarisation profiles rely on an external excitation of the material leading to a local change of material properties (Mellinger et al., 2007). A thermal excitation in terms of thermal waves or thermal pulses gives rise to a pyroelectric current, which carries information on the polarisation profile. In the frequency domain, the laser intensity modulation method (LIMM) is well-established. Thereby temperature oscillations are generated by a periodically modulated laser beam (Lang and Das-Gupta, 1986). When thermal pulses are applied with a pulsed laser, the signal is recorded in the time domain (Collins, 1977). The advantage of the thermal pulse method is a higher pyroelectric signal in a shorter measuring time. In Pham et al. (2009) both methods are used to map the polarisation profiles in thin dielectric films with a high resolution. Pham et al. (2009) came to the conclusion that they provide similar results with the thermal pulse method being up to 50 times faster. The use of scanning LIMM to generate a polarisation map of the sample surface is described in more detail by Stewart and Cain (2009). In Stewart and Cain (2015), piezoelectric films of thicknesses down to 100 nm are measured with high-frequency LIMM.

In this work, we present simplified analytical and numerical finite element models to describe the pyroelectric response of the LIMM and the thermal pulse method, and we compare them to experimental results.

2 Theory

The pyroelectric current is described by a fundamental relation:

$$I(t) = \frac{A}{d} \int_0^d p(z) \frac{\partial}{\partial t} \Theta(z,t) \mathrm{d}z, \tag{1}$$

where A is the heated area, d the piezoelectric film thickness, $p(z)$ the pyroelectric coefficient distribution, and $\Theta = T - T_0$ the temperature difference to the environment.

Assuming a homogeneous polarisation equivalent to $p(z) = p_0 = \text{const.}$, Eq. (1) simplifies to

$$I(t) = \frac{A}{d} p_0 \int_0^d \frac{\partial}{\partial t} \Theta(z,t) \mathrm{d}z = A p_0 \frac{\mathrm{d}\Theta_m}{\mathrm{d}t}, \tag{2}$$

where $\Theta_m(t)$ is the temperature averaged across the sample.

In this work, we use different models to determine the temperature distribution $\Theta(z,t)$ and the resulting pyroelectric current.

2.1 Laser intensity modulation method

In the case of LIMM, we consider a harmonically heated piezoelectric plate exhibiting heat losses to the environment, characterised by a thermal relaxation time τ_{th} (Suchaneck et al., 2012). The steady-state periodic solution of this problem in the form of an infinite series is given by Bauer and Ploss (1990) and Carslaw and Jaeger (1959):

$$\Theta(z,t) = \frac{\Phi_0}{c\rho \cdot d} \left[\frac{\tau_{\mathrm{th}}}{1+i\omega\tau_{\mathrm{th}}} + 2 \cdot \sum_{n=1}^{\infty} \cos\left(\frac{n\pi \cdot z}{d}\right) \frac{\tau_{\mathrm{d}}/n^2}{1+i\omega\tau_{\mathrm{d}}/n^2} \right] \exp(i\omega t), \tag{3}$$

where Φ_0 is the heat flux absorbed by the plate surface, c the specific heat, ρ the density, $\tau_{\mathrm{d}} = d^2/\pi^2 a$ the heat diffusion time, and a the thermal diffusivity of the plate. The pyroelectric response then yields (Bauer and Ploss, 1990)

$$I(\omega) = \frac{\Phi_0 A}{c\rho \cdot d} \left(p_0 \frac{i\omega\tau_{\mathrm{th}}}{1+i\omega\tau_{\mathrm{th}}} + \sum_{n=1}^{\infty} p_n \frac{i\omega\tau_{\mathrm{d}}/n^2}{1+i\omega\tau_{\mathrm{d}}/n^2} \right) \exp(i\omega t), \tag{4}$$

where p_0 is the average pyroelectric coefficient and p_n are its spatially dependent parts.

For a continuous distribution of relaxation times (instead of a single time constant) and a homogeneous polarisation with $p_n = 0$, Eq. (4) results in (Suchaneck et al., 2013)

$$I(\omega) = \frac{\Phi_0 A}{c\rho \cdot d} p_0 \left[1 - \frac{1}{\left[1+(i\omega\tau_{\mathrm{th}})^{\alpha}\right]^{\beta}} \right] \exp(i\omega t). \tag{5}$$

This model is equivalent to the Havriliak–Negami function as known from dielectric relaxation with the empirical parameters α and β accounting for the broadness and asymmetry of the distribution function. Two special cases are the Cole–Cole relaxation for $\beta = 1$ and $\alpha < 1$ and the Cole–Davidson relaxation for $\alpha = 1$ and $\beta < 1$.

Depending on the sample design, a superposition of several relaxation processes is also possible.

2.2 Thermal pulse method

2.2.1 Analytical solution

The temperature distribution after heating the piezoelectric plate by a laser pulse can be described by a transient pulse model of Camia (1967). It assumes an infinitely short laser pulse, a thermally isolated top surface and thermal coupling of the backside to an ideal heat sink. The temperature distribution is given by an infinite series of exponential terms:

$$\Theta(\xi,\tau) = \sum_{m=0}^{\infty} 2\cos\left[\frac{(2m+1)\pi}{2}\xi\right] \exp\left[-\frac{(2m+1)^2\pi^2}{4}\tau\right]. \tag{6}$$

$\xi = z/d$ and $\tau = at/d^2$ are dimensionless variables of depth and time, respectively. Inserting Eq. (6) in Eq. (2) yields for the time-dependent pyroelectric current:

$$I(\tau) = -A p_0 \frac{a}{d^2} \sum_{m=0}^{\infty} (2m+1)\pi \cdot (-1)^m \exp\left[-\frac{(2m+1)^2\pi^2}{4}\tau\right]. \tag{7}$$

Another analytical approach is a one-dimensional transient heat transfer model introduced by Bloß et al. (2000). It additionally considers the thermal mass of the electrode. The temperature distribution yields

$$\Theta(\xi,\tau) = \sum_{k=0}^{\infty} 2 \frac{\sin[x_k(1-\xi)]}{(1+r+r^2x_k^2)\sin x_k} \exp(-x_k^2\tau), \tag{8}$$

where r is the ratio of the thermal mass of the electrode to that of the pyroelectric element. x_k are the solutions of a transcendent equation, which is solved numerically. The resulting pyroelectric current is given by

$$I(\tau) = -A p_0 \frac{2a}{d^2} \sum_{k=0}^{\infty} 2 \frac{x_k(1+\cos x_k)}{(1+r+r^2x_k^2)\sin x_k} \exp(-x_k^2\tau). \tag{9}$$

2.2.2 Numerical solution

The temperature distribution was also determined by a finite element model (FEM) solved by ANSYS 15.0.

The transient thermal analysis was performed by applying a heat flux in the area of the laser spot on the top of the sample for the duration of the laser pulse (0.5 µs). The backside of the sample was assumed to be an ideal heat sink. The initial temperature of the device was set to 20 °C. The material properties used for modelling are listed in Table 1.

Table 1. Material properties of the PZT plate (PI Ceramic GmbH, 2015).

Density, $\mathrm{g\,cm^{-3}}$	Thermal conductivity, $\mathrm{W\,m^{-1}\,K^{-1}}$	Specific heat, $\mathrm{J\,kg^{-1}\,K^{-1}}$
7.8	1.1	350

3 Experimental methods

Two different types of embedded piezoelectric transducers were evaluated:

i. A low-temperature co-fired ceramics (LTCC)/lead–zirconate–titanate (PZT) sensor and actuator consisting of an already sintered PZT plate (CeramTec Sonox® P53) with a size of $(25 \times 10 \times 0.2)\,\mathrm{mm}^3$ embedded in the centre of a sintered LTCC module ($(45 \times 20 \times 0.7)\,\mathrm{mm}^3$, Heraeus HeraLock® Tape-HL2000). Sample fabrication is described in detail elsewhere (Flössel et al., 2010). The sample capacitance was 30 nF, the dielectric loss tangent amounted to about 2 % at 10 kHz.

ii. A commercial M-8528-P2 macro-fibre composite (MFC) actuator (Smart Materials, Dresden, Germany) with an overall length of 105 mm, an active length of 85 mm, an active width of 28 mm, a thickness of about 0.3 mm, a sample capacitance of 170 nF, and a dielectric loss tangent of about 5 % at 10 kHz. PZT macro-fibres are embedded in epoxy resin. They are electrically contacted by copper electrode strips and covered by a Kapton film.

In comparison, a non-embedded PZT plate with a size of $(10 \times 7 \times 0.2)\,\mathrm{mm}^3$ covered by a nickel–chromium electrode was analysed.

For LIMM measurements, the samples were periodically heated by an array of six laser diodes or a single laser diode (LCU98A041A, Laser Components GmbH, Olching, Germany) square-wave modulated with frequencies of up to 1 kHz each with a power of 14 mW at a wavelength of 980 nm. The complex pyroelectric current was determined by an impedance/gain-phase analyser (Solartron 1260, Solartron Analytical, Farnborough, UK) with DC coupling. In order to reduce noise, 30 measurement repetitions were used for averaging.

Thermal pulse measurements were carried out by heating the samples with a pulsed laser diode (LC905D1S3J09UA, Laser Components GmbH, Olching, Germany) at a wavelength of 905 nm with a maximal peak power of 75 W, a pulse width of 0.15 or 0.5 µs and a repetition frequency of 1 Hz. The pyroelectric current was transformed to a voltage by a current amplifier (DLPCA-200, Femto Messtechnik GmbH, Berlin, Germany) and the signal was recorded by a Waverunner® Xi-A oscilloscope (LeCroy, Chestnut Ridge, USA).

4 Results and discussion

4.1 Laser intensity modulation method

Figure 1 shows the pyroelectric current spectrum of the non-embedded PZT plate fitted to Eq. (5). The thermal relaxation time amounts to 0.8 s. The fit shows a deviation from an ideal Debye-like model due to a slight time distribution, which is attributed to the impact of the electrodes and the electrical contact by a wire. The spectrum is best described by a Cole–Davidson relaxation with $\beta = 0.9$. The PZT plate shows a homogeneous polarisation distribution. The obtained

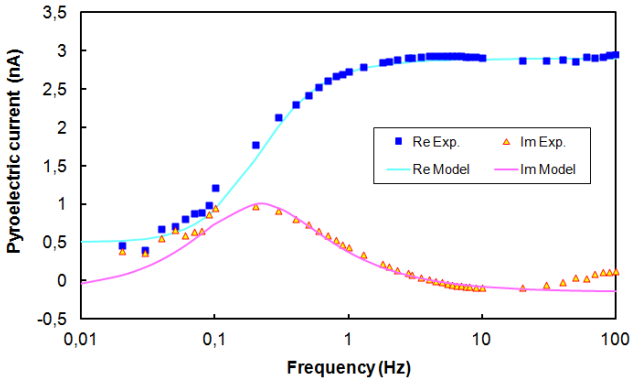

Figure 1. Pyroelectric current spectrum of a PZT plate in comparison to a fit to Eq. (5).

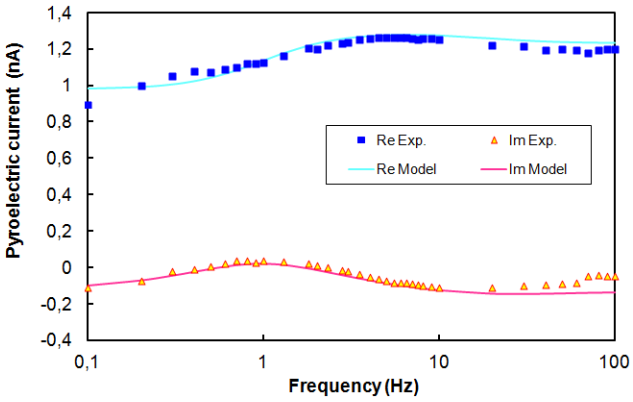

Figure 2. Pyroelectric current spectrum of a LTCC/PZT sensor–actuator in comparison to a fit to Eq. (4) with $p_1 = -p_0/5$.

pyroelectric spectrum is comparable to the results of Bauer and Ploss (1990). Note that the analytical model of Bauer and Ploss (1990) was originally developed for non-embedded samples. The following demonstrates that this model can be successfully applied to embedded piezoelectric transducers.

Figure 2 illustrates the pyroelectric current spectrum of a LTCC/PZT module fitted to Eq. (5). Between 0.1 and 10 Hz the embedded PZT plate loses heat to the LTCC layers with a thermal relaxation time of 0.16 s. A minor decrease of the real part at higher frequencies is attributed to a slightly inhomogeneous polarisation distribution, which is taken into account by $p_1 = -p_0/5$. A detailed analysis was previously reported by Eydam et al. (2014).

The MFC actuator is an example for a broad relaxation time distribution, which is well described by a Cole–Cole function with $\alpha = 0.4$ (Fig. 3). The relaxation time constant with a value of 5.3 s describes the heat loss of the sample surface to the environment with a thermal conductance of about $100\,\mathrm{W\,m^{-2}\,K^{-1}}$. Here, the pyroelectric current spectrum is satisfactorily modelled by assuming a homogeneous polarisation.

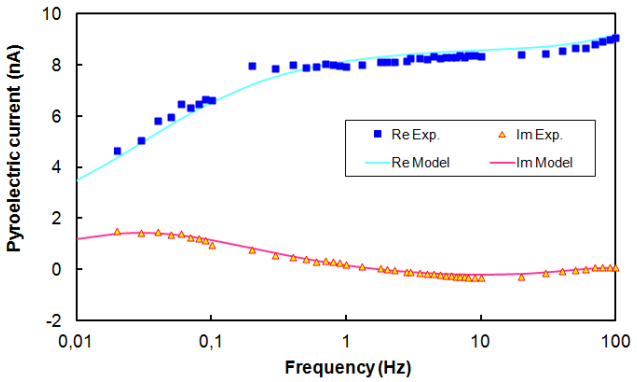

Figure 3. Pyroelectric current spectrum of a MFC actuator in comparison to a fit to Eq. (5).

4.2 Thermal pulse method

4.2.1 Modelling results

The mean temperature of the sample and the resulting pyroelectric current were determined for the PZT plate with the analytical models and the FEM model as described above.

Figure 4 illustrates the mean temperature over a time period of 0.1 s. The analytical models start at the temperature maximum whereas the FEM model shows the increase of the temperature from room temperature to a maximum value since the laser pulse has a given time duration of 0.5 µs. The model of Bloß et al. (2000) does not reach the maximum immediately but shows a slight increase of the temperature at the beginning due to the thermal mass of the electrode. At longer times, the temperature decreases exponentially to room temperature. The heat diffusion time amounts to 0.01 s for the PZT plate; i.e. it is located shortly after the temperature maximum. At this point, the plate has reached an inner thermal equilibrium. On the other hand, the thermal relaxation time of 0.8 s is the point when the sample reverts to thermal equilibrium with its environment.

The pyroelectric current is proportional to the time derivative of the mean temperature of the sample presented in Fig. 5 (cf. Eq. 2). In the analytical models, the current starts at a very high positive value caused by initial heating and falls down almost immediately to a negative value. On the other hand, the FEM model illustrates additionally the rise of the positive current during the heating period (cf. Fig. 5b). After reaching a minimum the current slowly returns to zero in all models; i.e. the sample returns to steady-state conditions.

4.2.2 Experimental results

Figures 6 and 7 illustrate the measured pyroelectric current of the PZT plate and of the LTCC/PZT module and the MFC actuator. There is a short initial negative peak followed by a large positive signal.

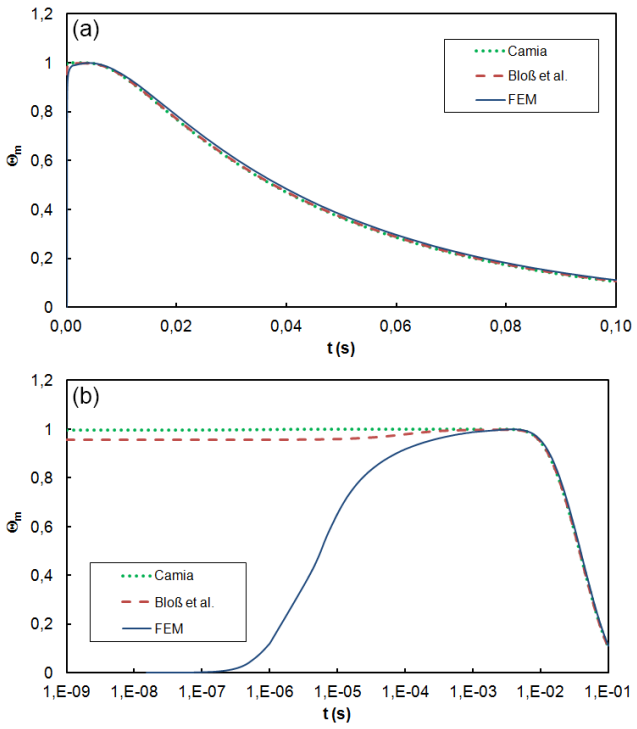

Figure 4. Mean temperature within a PZT plate, determined by three different models (cf. Sect. 2.2) with **(a)** linear and **(b)** logarithmic time axis.

Figure 6 illustrates that a longer pulse width leads to a higher heat input and thus a larger signal. The experimental data in Fig. 6 are in qualitative agreement with the simulation in Fig. 5b. Consequently, the experimental results manifest the initial heating of the piezoelectric plate. However, there is still a time shift between the signal maxima of the model and the experiment. One reason could be the thermal buffering effect of the top electrode (Bloß et al., 2000). It absorbs thermal energy during the short thermal pulse but only slowly transfers it to the piezoelectric since the heat transfer is limited by the piezoelectric's thermal diffusivity. Another reason could be the neglect of the rise and decay times of the laser pulse in the simulation. Both effects are now subject of further research. On the other hand, the signal of the cooling period at longer times is still too noisy for a quantitative analysis. Due to the very high gain of the current amplifier, mainly noise is present in the measured signal for measurement times of more than 0.5 ms. The signal shape is similar to the thermal pulse response of electret polymers obtained in Mellinger et al. (2005), where the high-gain signal decreases to zero for times exceeding 1 ms. For further measurements, a low-pass filter and a 50 Hz notch filter will be used to reduce the noise contribution.

In Fig. 7, the time shift of the maximum signal for the embedded piezoelectric plates is suspected to be caused by the heat transfer time through the embedding top layer. The

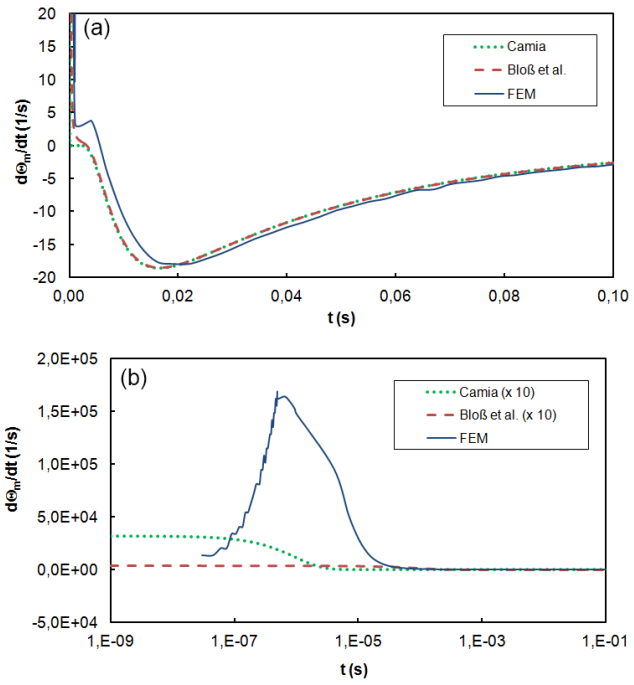

Figure 5. Time derivative of the mean temperature (proportional to the pyroelectric current) within a PZT plate, determined by three different models (cf. Sect. 2.2) with **(a)** linear and **(b)** logarithmic time axis. In **(b)** the values of the models of Camia (1967) and Bloß et al. (2000) were magnified by a factor of 10.

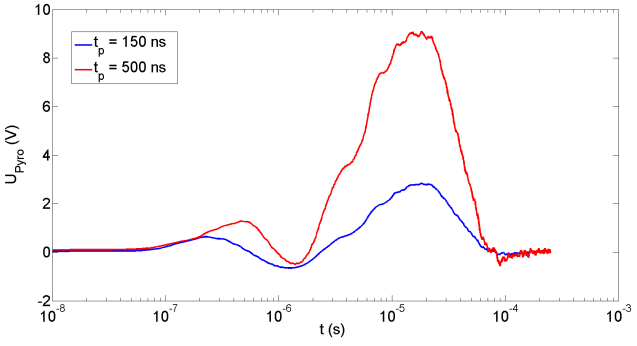

Figure 6. Time dependence of the output voltage of the current amplifier (10^8 V A^{-1}, 7 kHz bandwidth) for the PZT plate for an optical power of 22.5 W and a pulse width of 150 and 500 ns, respectively.

attenuation of the absorbed heat in the top layer would result in a smaller maximum of the pyroelectric signal.

5 Conclusions

The pyroelectric response of an embedded piezoceramic plate for the LIMM has been described by an analytical model, which was successfully applied to integrated sensor–actuator modules. For the thermal pulse method, the temperature distribution and the resulting pyroelectric current have been characterised both by two analytical and one FEM model. Further improvement of the thermal pulse set-up is required to reduce the signal-to-noise ratio in the cooling period. In the next step, a Fourier transform will be performed to analyse the thermal pulse signal in the frequency domain. This enables the application of the LIMM models to a signal that was recorded in a much shorter measuring time.

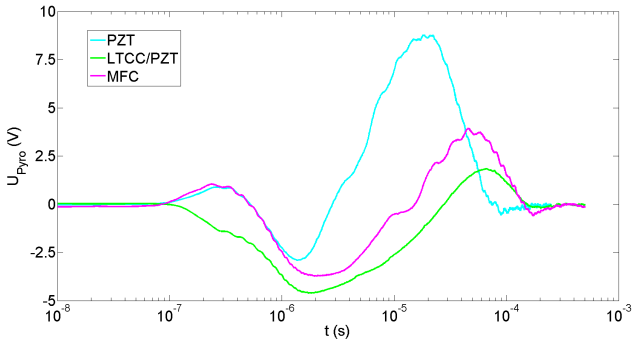

Figure 7. Time dependence of the output voltage of the current amplifier (10^8 V A^{-1}, 7 kHz bandwidth) for the PZT plate, the LTCC/PZT sensor–actuator and the MFC actuator for an optical power of 65 W and a pulse width of 150 ns.

Acknowledgements. This research is supported by the Deutsche Forschungsgemeinschaft (DFG) in context of the Collaborative Research Centre/Transregio 39 PT-PIESA, subproject C8.

Edited by: A. Schütze
Reviewed by: two anonymous referees

References

Bauer, S. and Ploss, B.: A method for the measurement of the thermal, dielectric, and pyroelectric properties of thin films and their applications for integrated heat sensors, J. Appl. Phys., 68, 6361–6367, 1990.

Bloß, P., DeReggi, A. S., and Schäfer, H.: Electric-field profile and thermal properties in substrate supported dielectric films, Phys. Rev. B, 62, 8517–8530, 2000.

Camia, F. M.: Traité de Thermocinétique impulsionelle, Dunod, Paris, 1967.

Carslaw, H. S. and Jaeger, J. C.: Conduction of Heat in Solids, 2nd edn., Oxford University Press, New York, NY, 1959.

Collins, R. E.: Measurement of charge distribution in electrets, Rev. Sci. Instrum., 48, 83–91, 1977.

Eydam, A., Suchaneck, G., Esslinger, S., Schönecker, A., Neumeister, P., and Gerlach, G.: Polarization characterization of PZT disks and of embedded PZT plates by thermal wave methods, in: AIP Conference Proceedings 1627, Electroceramics XIV, Bucharest, Rumania, 16–20 June 2014, 31–36, 2014.

Flössel, M., Gebhardt, S., Schönecker, A., and Michaelis, A.: Development of a novel sensor-actuator-module with ceramic mul-

tilayer technology, Journal of Ceramic Science and Technology, 1, 55–58, 2010.

Lang, S. B. and Das-Gupta, D. K.: Laser-intensity-modulation method, a technique for determination of spatial distributions of polarization and space charge in polymer electrets, J. Appl. Phys., 59, 2151–2160, 1986.

Mellinger, A., Singh, R., and Gerhard-Multhaupt, R.: Fast thermal-pulse measurements of space-charge distributions in electret polymers, Rev. Sci. Instrum., 76, 013903, doi:10.1063/1.1832153, 2005.

Mellinger, A., Singh, R., Wegener, M., Wirges, W., and Gerhard-Multhaupt, R.: Zerstörungsfreie Tomographie von Raumladungs- und Polarisationsverteilungen mittels Wärmepulsen (Non-destructive Space-charge and Polarization Tomography with Thermal Pulses), Tech. Mess., 74, 437–444, 2007.

PI Ceramic GmbH: Werkstoffdaten, Spezifische Parameter der Standardmaterialien, available at: http://www.piceramic.de/download/PI_Ceramic_Werkstoffdaten.pdf, last access: 17 August 2015.

Pham, C.-D., Petre, A., Berquez, L., Flores-Suárez, R., Mellinger, A., Wirges, W., and Gerhard, R.: 3D high-resolution mapping of polarization profiles in thin Poly(vinylidenefluoride-trifluoroethylene) (PVDF-TrFE) films using two thermal techniques, IEEE T. Dielect. El. In., 16, 676–681, 2009.

Stewart, M. and Cain, M.: Use of scanning LIMM (Laser Intensity Modulation Method) to characterise polarization variability in dielectric materials, J. Phys. Conf. Ser., 183, 012001, doi:10.1088/1742-6596/183/1/012001, 2009.

Stewart, M. and Cain, M.: Using High Frequency LIMM to characterize the poling state of piezoelectric ceramic thin films, MRS Proceedings 1805, 2015.

Suchaneck, G., Eydam, A., Hu, W., Krantz, B., Drossel, W.-G., and Gerlach, G.: Evaluation of polarization of embedded piezoelectrics by the thermal wave method, IEEE T. Ultrason. Ferr., 59, 1950–1954, 2012.

Suchaneck, G., Eydam, A., and Gerlach, G.: A laser intensity modulation method for the evaluation of the polarization state of embedded piezoceramics, Ferroelectrics, 453, 127–132, 2013.